

RSC Advances



This is an *Accepted Manuscript*, which has been through the Royal Society of Chemistry peer review process and has been accepted for publication.

Accepted Manuscripts are published online shortly after acceptance, before technical editing, formatting and proof reading. Using this free service, authors can make their results available to the community, in citable form, before we publish the edited article. This *Accepted Manuscript* will be replaced by the edited, formatted and paginated article as soon as this is available.

You can find more information about *Accepted Manuscripts* in the [Information for Authors](#).

Please note that technical editing may introduce minor changes to the text and/or graphics, which may alter content. The journal's standard [Terms & Conditions](#) and the [Ethical guidelines](#) still apply. In no event shall the Royal Society of Chemistry be held responsible for any errors or omissions in this *Accepted Manuscript* or any consequences arising from the use of any information it contains.

Cite this: DOI: 10.1039/c0xx00000x
www.rsc.org/xxxxxx

Engineered elastomeric bio-nano composites from linseed oil/organoclay tailored for vibration damping

Rakesh Das,^a Rajesh Kumar,^b Sovan Lal Banerjee^a and P. P. Kundu^{a*}

Received (in XXX, XXX) Xth XXXXXXXXX 20XX, Accepted Xth XXXXXXXXX 20XX

DOI: 10.1039/b000000x

This study deals with the preparation and characterization of elastomeric nano composites from renewable resources for vibration damping applications. The nano composites were synthesized by in situ cationic polymerization technique in the presence of organophilic montmorillonite (modified nano clay) filler. The clay filled nano composites showed superior dynamic moduli in comparison with the pure elastomers. The storage modulus at room temperature (25 °C) was improved by 1.56 to 2 times with respect to pure elastomers with an increase in the filler content from 1 to 4 %. A good and stable vibration damping is observed in a wide temperature and frequency region (1-50 Hz). The loss factor, $\tan \delta_{\max}$ obtained from dynamic mechanical analysis varies from 0.58 to 0.87. Under laboratory fabricated testing system, the transient attenuation with the complete decay of applied vibration within nano composites demonstrates that the elastomeric nanocomposites have the potential as effective damping materials.

Introduction

In recent years, there is a growing interest in renewable plant based materials over petroleum-derived raw materials for production of polymeric materials and composites because of increasing environmental awareness and necessity for carbon fixation¹. Natural oils are versatile renewable resources for producing functional polymeric materials²⁻⁵ because of their low production cost, universal availability and biodegradability. Reinforcing polymers with organic or inorganic fillers is a common practice in polymer industry to improve mechanical stability, thermal stability, improve barrier properties, enhancement of flame retardancy and reduction of production cost⁶⁻⁸. Polymer nano composites have captured intense attention over the traditional composites reinforced with high amount of inorganic fillers in different engineering applications⁹⁻¹². The nano reinforcement has been utilized for the preparation of advanced composite materials with balanced properties. Due to nano-scale dimension of the filler in polymer nano composites, the interfacial interaction of the fillers with polymer matrix increases tremendously. This leads to a significant improvement in composite properties even at a very low volume fraction of filler loading¹³.

Larock et al.^{14, 15} have produced a variety of polymers by direct polymerization of native natural oil with styrene (ST) and divinylbenzene (DVB) initiated by cationic initiator, boron trifluoride diethyl etherate (BFE). Wool et al.^{3, 16} have synthesized rubbers, rigid composites and adhesives through free radical polymerization from chemically modified oil. Petrovic et al.^{17, 18} have developed polyurethanes from soy polyols derived from epoxidized vegetable oils. In recent years, polymers have been synthesized from vegetable oils by relatively new polymerization techniques like acrylic metathesis polymerization

(ADMET)¹⁹ and ring-opening metathesis polymerization (ROMP)^{20, 21}. Polymeric composites/ nano composites have been prepared by reinforcing vegetable oil-based polymers with fillers or fibers depending on specific applications²². Composites have found promising applications in automobile, aircraft, defence packaging etc. Natural oil based polymer-silicate nano composites containing very low level of exfoliated/ intercalated clay such as montmorillonite and vermiculite have attracted considerable attention because of dramatic enhancement of their properties with respect to virgin polymers²³⁻²⁵. For nano composites preparation, clays has been focused and studied the most since they are naturally occurring materials having the nano layers morphology with very high aspect ratio and surface area²⁶. The fibers are also utilized as a reinforcing agent in natural oil based polymers to prepare composites or nano composites with improved mechanical properties^{27, 28}. Larock et al. have performed a lot of research work to prepare bio-composites from conjugated linseed or soybean oil based resins filled with different natural fibers like wheat straw, wood fiber, rice hull and switch grass etc²⁹⁻³².

Polymeric materials have useful applications as a vibration damper where vibration and its efficient control are prime concern for product designers in machinery, structural engineering and dynamic systems. In a previous work, we developed elastomers from linseed oil and its vibration damping properties and mechanical properties were analyzed³³⁻³⁴. Linseed oil is the most abundant and cheap non edible oil among different natural oils³³. In the present research work, the elastomeric nano-composites with enhanced mechanical stability and vibration damping properties have been developed from linseed oil reinforced with organically modified clay. Thus, the prime objective of this work is the development of value added nano composites having potential engineering applications from cheap

bio-renewable resources. The morphology of the nano-composites has been studied through a scanning electron microscope (SEM) for the investigation of filler-matrix internal adhesion which is a very important parameter controlled the mechanical and viscoelastic properties of composites³⁵. The polymeric materials are very effective vibration damping materials owing to their viscoelastic behaviour³⁶. Thus the viscoelastic parameters like storage modulus, loss modulus, damping loss factor etc are analyzed for systematic performance analysis of nano-composites in vibration damping applications. As the low frequency vibration like earthquake, wind induced vibration, track vibration, vibration in machinery etc are very much harmful for human being, the low frequency vibration damping properties of these nano composites have been evaluated by a laboratory fabricated testing system for their suitability in practical vibration damping applications.

Experimental

Materials

Linseed oil used in our study was obtained from the local market of Kolkata. Iodine value and acid value of linseed oil were determined as 178 g I₂/100g and 0.6 mg KOH/ g oil respectively. Styrene (ST), divinylbenzene (DVB) (55 mole % DVB and 45 mole % ethylvinylbenzene) and boron trifluoride diethyl etherate complex were purchased from Sigma-Aldrich, USA. Montmorillonite (K-10) (MMT) and cetyl trimethyl ammonium bromide (CTAB) were purchased from Aldrich Chemical Company, USA.

Modification of Montmorillonite

MMT clay was dispersed in deionised (DI) water by stirring. CTAB is added to dispersion. The whole dispersion was heated at 60 °C for 6 hrs with a constant stirring condition. This solution was centrifuged at 8000 rpm for 3 min. The modified MMT solution was washed repeatedly and filtered until no precipitate appeared after addition of AgNO₃ solution (0.1 mol/lit) into the filtrate. The filtered cake was dried in vacuum at 80°C for 12 hrs and then grounded it using mortar and pestle to obtain the fine powder of organically modified clay (OMMT). The OMMT was further characterized by fourier transform infrared spectroscopy (FTIR), dynamic light scattering (DLS) and X-ray diffraction (XRD).

Nanocomposite Preparation

The desired amount of ST and DVB were added to the linseed oil and the modified MMT was dispersed with this mixture. The dispersion was maintained by constant magnetic stirring at 600 rpm for 24 hrs followed by mild ultrasonication for 30 min for proper intercalation. Then, the mixture was cooled in ice bath and initiator was added slowly in a vigorous stirring condition. The BFE initiator was modified by mixing of 5 wt % initiator with 10 wt % methyl ester of linseed oil to ensure a homogeneous polymerization during its subsequent use as initiator. Methyl ester was prepared in two consecutive steps in a transesterification process³⁷. Instead of regular linseed oil, the methylester of linseed oil was used for better miscibility with initiator which caused the uniform distribution of initiator in

reaction mixtures. After homogeneous mixing, the resulting mixture was transferred in to a glass mold and the mold was properly sealed with silicon adhesives. The mold was kept at room temperature for 2 hrs and then it was heated sequentially at 60 °C to 80 °C for 2 hrs, 110 °C for 12 hrs, finally post cured at 120 °C for 3 hrs. The fixed matrix composition was 40 wt % of linseed oil, 27 wt % of ST, 18 wt % of DVB and 15 wt % of initiator. The modified MMT loading into the fixed matrix was varied from 0 to 5 wt % to get a variety of elastomeric nano composites. A schematic of preparation of nano composites is shown in Figure 1.

Characterization

Dynamic light scattering (DLS)

The average particle size and particle size distribution of the water dispersed MMT and modified MMT were determined by means of dynamic light scattering (DLS) performed at 25 °C on a Zetasizer Nano ZS 90 (Malvern, UK) light scattering instrument at an scattering angle of 90°.

X ray Diffraction (XRD) Analysis

X-ray diffraction spectrometry of the MMT, modified MMT and nanocomposites were performed by a wide angle X-ray scattering diffractometer (Panalytical X-Ray Diffractometer, model- X'pert Powder) with Cu K_α radiation ($\lambda=0.154$ nm) in the range of 4–35° (2 θ) at 40kV and 30mA.

Fourier Transform Infrared Spectroscopy (FTIR)

The modified MMT and nano composites were analyzed by attenuated total reflectance (ATR) method of FTIR. A total of 42 scans at 4 cm⁻¹ resolution in transmittance mode were performed by a FTIR spectrophotometer (Model: Alpha-E, Bruker, Germany) to get an average spectrum.

Field Emission Scanning Electron Microscopy Analysis (FESEM)

In order to determine the microstructure of polymer-clay nano composites, the field emission scanning electron microscope (JEOL JSM-7600F) was utilized with an acceleration voltage of 5 kV. Prior to scanning, the samples were sputter coated with a thin layer (approximately 25 nm) of gold under vacuum by using an Ion sputter coater of Hitachi, Japan (Model:E1010).

Dynamic Mechanical Analysis

The dynamic mechanical properties of the nano composites were measured using a dynamic mechanical analyzer (Perkin Elmer DMA 8000). A rectangular specimen of dimension 10 mm × 5 mm × 2 mm was tested in strain controlled compression mode at a fixed frequency of 1 Hz and dynamic strain of 0.001 % in the temperature range of -30 °C to 60 °C with a rate of increase in temperature of 5 °C/ min. The storage modulus (E'), loss modulus (E'') and damping loss factor ($\tan \delta$), which is the ratio of E'' and E' were recorded as a function of temperature. The variation of E' and $\tan \delta$ was optimized with the varying content of clay in different samples. The frequency sweep of storage modulus (E'), loss modulus (E'') and loss factor ($\tan \delta$) were

Cite this: DOI: 10.1039/c0xx00000x
www.rsc.org/xxxxxx

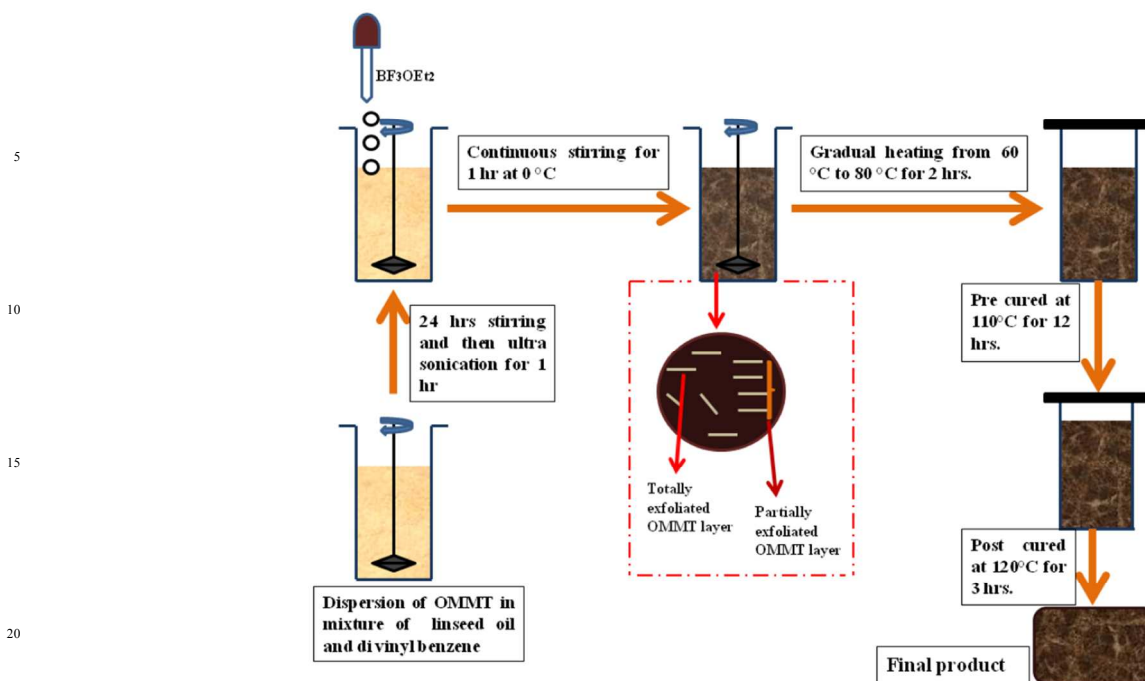


Fig. 1 Schematic of polymerization reaction for nano composite preparation

performed in strain controlled compression mode of the dynamic strain of 0.0005 % and the frequency range of 1 Hz to 50 Hz at room temperature (25 °C).

Fabrication of experimental set up for vibration damping analysis of nano composites

A square test piece of mild steel and nano composites was tested by keeping free of the four ends of the test piece. The mild steel test piece was tested to validate the experimental set up and technique. The mild steel base plate was fabricated in the size of 100 × 100 × 2 mm having mass per unit area 16.5 kg/m². The elastomer was taken on the size of 100 × 100 × 3 mm. The test piece was excited at its top middle position by the sinusoidal excitation which was generated by the electrodynamic shaker of Modal Shop Inc., USA (Model K2004E01). The shaker was controlled by the function generator of Agilent Technologies, USA (Model 33220A). A sinusoidal waveform of 5 Hz fixed frequency and constant amplitude of 1.5 V (R.M.S) was applied with the help of this function generator. The response of the test piece was picked up from its middle position by the piezoelectric light weight accelerometer of Metra Mass-und Frequenztechnik, Germany (Model KS94B. 100*/01). The accelerometer was connected with a digital storage oscilloscope of Aplab Limited, India (Model D36100C) interfaced with the PC, where the resulting waveform is displayed. The schematic of the experimental set up, the excitation point and detection point of the test piece were shown in Figure 2. The time decay waveform of the test piece was recorded by the oscilloscope and the loss

factor was calculated by using this waveform. The loss factor was calculated by the logarithmic decrement method using the equation³⁸,

$$\eta = 2\zeta = 2 \frac{1}{\sqrt{1 + \left(\frac{2\pi}{\delta}\right)^2}} \quad (1)$$

where, δ is the logarithmic decrement, defined by

$$\delta = \frac{1}{r} \ln\left(\frac{A_i}{A_{i+r}}\right) \quad (2)$$

where, r is the number of cycles, ζ is the damping ratio, A_i is the first significant amplitude and A_{i+r} is the amplitude after r cycles.

Results & Discussions

Determination of particle size distribution of clay by DLS

From the DLS study, the Z-Average particle size of Na-MMT and CTAB modified MMT were obtained as 593 nm and 683 nm, respectively. The curve for the statistical particle size distribution versus scattered light intensity is shown in Figure 3. The Z-Average particle size of CTAB modified MMT is found to be higher than Na-MMT due to the incorporation of tertiary ammonium ion in the MMT structure.

XRD analysis

Cite this: DOI: 10.1039/c0xx00000x
www.rsc.org/xxxxxx

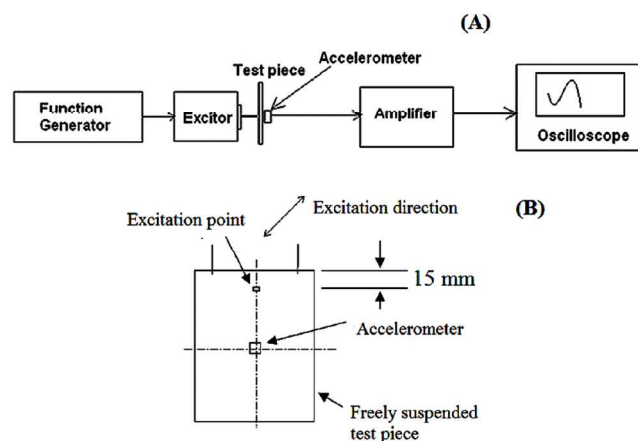


Fig. 2 A sketch of experimental set up for vibration response analysis of nano composites

The wide angle X-ray diffraction pattern for MMT, CTAB modified MMT and nano composites are shown in Figure 4.

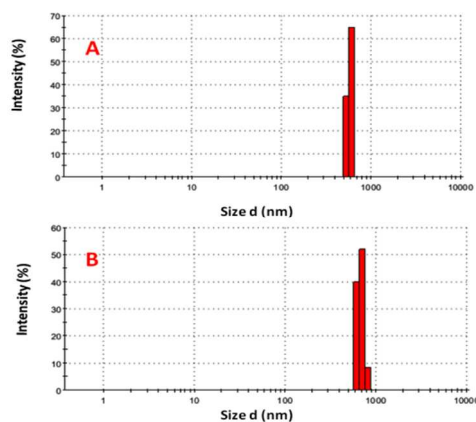


Fig. 3 DLS statistical size distribution of A. MMT & B. OMMT

MMT exhibits a strong diffraction peak at $2\theta = 6.04$ degree, corresponding to the interlayer spacing of (001) plane of MMT. Utilizing Bragg's law ($2d \sin \theta = \lambda$, where λ and θ are the wavelength of X-ray and diffraction angle, respectively), the d spacing was calculated as 1.46 nm. In CTAB modified MMT, a strong diffraction peak obtained at $2\theta = 5.37$ degree, where $d = 1.65$ nm. This means that silicate layers of MMT are effectively intercalated by CTAB cations, causing an increase in the d-spacing³⁹. The XRD pattern of the nanocomposites with 1 wt %, 2 wt % and 4 wt % of modified MMT loading are also shown in Figure 4. In the diffraction pattern of nano composites, the (001) diffraction peaks are feeble compared to the MMT and CTAB modified MMT. This confirms the distortion of ordered platy nano layers of MMT due to intercalation of polymer chains

into the nano layer galleries of modified MMT. The diffraction peaks of nanocomposites at $2\theta \approx 20.61$ degree are designated for the crystallites of linseed oil based elastomers. The peak intensity for crystallites decreases on increasing the filler content from 1 wt % to 5 wt % in the nano-composites.

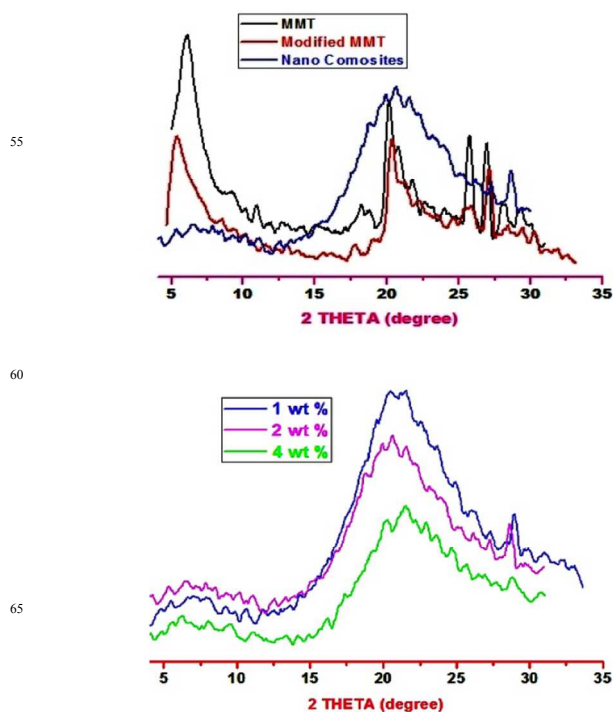


Fig. 4 XRD pattern of MMT, OMMT & nano composites

FTIR Spectroscopy analysis of Clay, modified Clay and Nanocomposites

The FTIR spectra of MMT, modified MMT, linseed oil and nano composites are shown in Figure 5. The analytical evaluation of FT-IR spectra are given in Table 1⁴⁰⁻⁴².

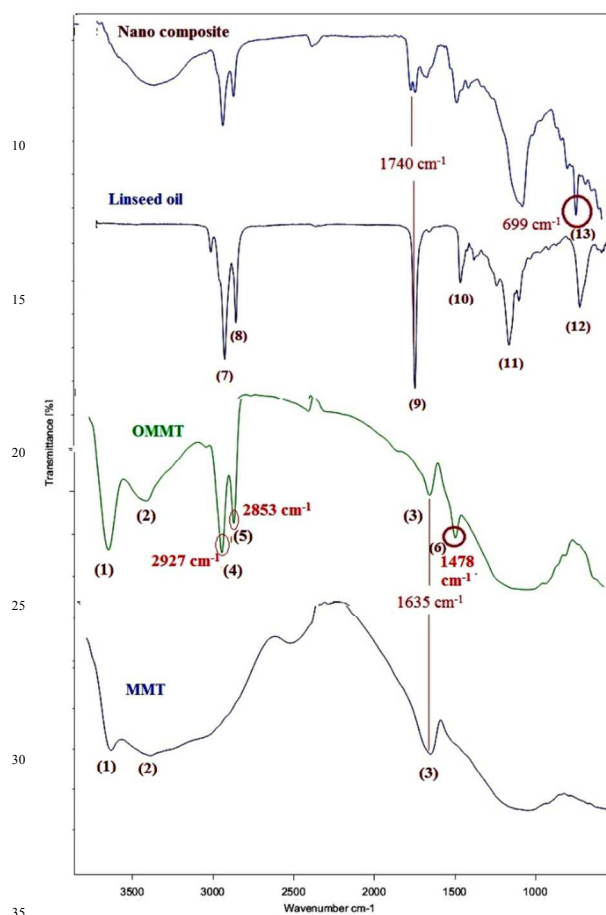


Fig. 5 FTIR spectra of MMT, OMMT, linseed oil & nano composites

In the FTIR spectrum of CTAB modified MMT, the absorption band at 1450 cm^{-1} due to the $-\text{CH}_3$ bending vibration mode of $\text{RN}(\text{CH}_3)_3^+$ ion of CTAB is the characteristic peak of modified MMT. The absorption bands at 3630 cm^{-1} and 3395 cm^{-1} are defined as the stretching vibration of free $-\text{OH}$ and bound $-\text{OH}$ of both MMT and CTAB modified MMT. In comparison to MMT, the band area for these two peaks increases in modified MMT, indicating the introduction of CTAB in MMT. The intensity of $-\text{OH}$ bending for the interlayer water of MMT at 1635 cm^{-1} decreases in modified MMT because the water content is reduced through the replacement of hydrated cations by surfactant cation ions. In the nano composite, the stretching vibration modes of ester linkage ($\text{C}=\text{O}$) of linseed oil at 1740 cm^{-1} is considered as the characteristic peak of linseed oil present in nano composites and out of plane bending of aromatic ring at 700 cm^{-1} as the characteristic peak of aromatic contents (ST and DVB) in nano composites.

Morphology Analysis of Nanocomposites

The field emission scanning electron micrograph (FESEM) of

polymeric nano composites containing 2, 3, 4 and 5 wt % nano clay are shown in Figure 6. In 2, 3 and 4 wt % nano clay filled nano composites, the uniform dispersion of clay platelets are observed throughout the matrix. In 4 wt % clay filled nano composites, a very low extent of agglomeration of nano clays are observed but in 5 wt % filled nano composites, agglomeration is widely spread in large extent throughout the whole matrix. In all nano-composites except for 5 wt % filled nano composites, the homogeneous morphology indicates the intercalation of polymer molecules into clay layers. The efficient adhesion between polymer matrix systems and modified nano clay arises due to the lower interfacial tension and better intermolecular specific attraction between cetylammmonium ions of modified clay and polymer matrix, leading to the formation of nano-composites. In the FESEM, relatively large numbers of nano platelets are distinctive in the higher nano clay filled nano composites. Figure 6D shows the presence of many islands of nano clay agglomeration (encircled in the figures) distributed in polymer matrix. Thus, the dispersion of MMT is poor in the polymer matrix and two phase morphology i.e. the tactoid structure is formed. This leads to a weaker interfacial bonding between the clay and matrix.

Dynamic mechanical analysis of nano composites

Under periodic excitation, the elastic part of any viscoelastic material stores energy where the viscous part dissipates energy according to the theory of viscoelasticity³⁶. The storage modulus is the amount of energy stored per cycle of excitation and it measures the elastic nature of the materials. The elastomer matrix of nano composites consists of two parts; the first one is the cross-linked polymer chain of ST-DVB on which linseed oil is grafted and the second one is the unreacted part comprising of free linseed oil, homo polymer of ST and DVB and a small proportion of copolymer of ST and DVB. The plasticized homopolymer contributes towards the viscous nature, whereas the cross-linked part elasticity though overall the whole network shows viscoelastic characteristics. The dangling chain ends have also effect on viscous property. The variation of E' and loss factor ($\tan \delta$) with temperature for different elastomers having varying clay contents is shown in Figure 7. The detailed dynamic mechanical analysis results are also reported in Table 2. The storage moduli of all samples are high at $-30\text{ }^\circ\text{C}$ and then a sharp decrease is observed between $6\text{ }^\circ\text{C}$ $-40\text{ }^\circ\text{C}$, corresponding to a primary relaxation process followed by a rubbery plateau region after $40\text{ }^\circ\text{C}$. The storage modulus decreases for all samples in the primary relaxation process where $\tan \delta$ goes through the maximum. From the storage modulus versus temperature plot, it is observed that with respect to the pure elastomer, the storage modulus increases with an increase in the clay content. This nature of storage modulus establishes the reinforcing capability of modified nano clay. During the primary relaxation process, the storage modulus of pure elastomers decreases more steeply than the nano composites. With an increase in temperature up to $100\text{ }^\circ\text{C}$, a steady improvement of storage modulus is monitored. Thus, it is proved that the presence of filler improves the rigidity and thermal stability of elastomers.

The variations of storage modulus with an increase in clay content in elastomers matrix for three different temperatures are plotted in Figure 7.

Cite this: DOI: 10.1039/c0xx00000x
www.rsc.org/xxxxxx

Table 1 Evaluation of FTIR spectra

| Wave number (cm ⁻¹) | Assignments |
|---------------------------------|--|
| ≈3630 (1) | Stretching vibration mode of free hydroxyl (-OH) group of MMT and CTAB modified MMT |
| ≈3395 (2) | Stretching vibration mode of hydrogen bonded hydroxyl group (-OH) of MMT and CTAB modified MMT |
| ≈1635(3) | -OH bending of interlayer water of MMT |
| ≈2927 (4) | Asymmetric stretching vibration modes of methylene group (-CH ₂) of long aliphatic tail of CTAB |
| ≈2853(5) | Symmetric stretching vibration modes of methylene group(-CH ₂) of long aliphatic tail of CTAB |
| ≈1478(6) | -CH ₃ bending of RN(CH ₃) ₃ ⁺ ion of CTAB |
| ≈2900 (7) | Asymmetric stretching vibration modes of methylene group (-CH ₂)of linseed oil |
| ≈2850 (8) | Symmetric stretching vibration modes of methylene group of linseed oil |
| ≈1740 (9) | Stretching vibration modes of ester linkage (C=O) of linseed oil |
| ≈1450 (10) | Asymmetric bending vibration modes of methylene group of linseed oil |
| ≈1150 (11) | Stretching vibration of ether linkage (C-O-C) of linseed oil |
| ≈720 (12) | Overlapping of -CH ₂ rocking vibration and out-of-plane vibration of <i>cis</i> -disubstituted olefins of linseed oil |
| ≈700 (13) | Out of plane bending vibration of aromatic ring of styrene and divinylbenzene |

^a

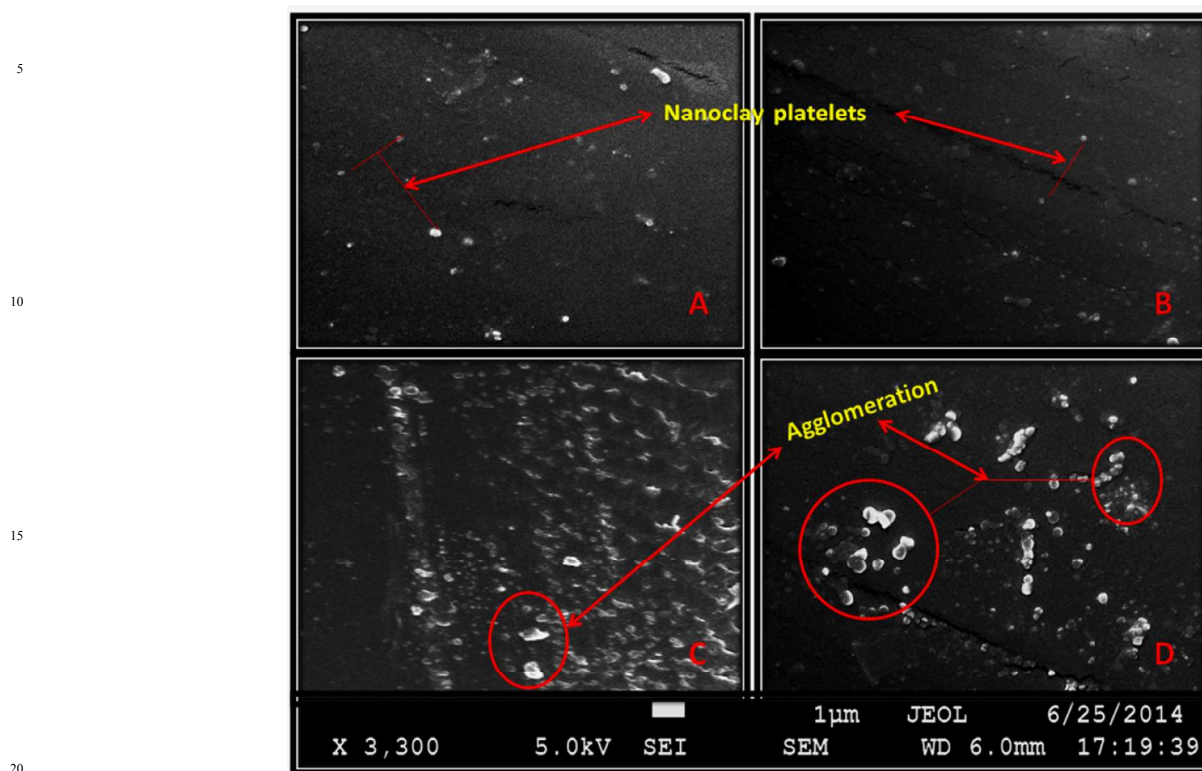


Fig.6 FESEM micrograph of nano composites of nano clay content **A.** 2 wt %, **B.** 3 wt %, **C.** 4 wt % & **D.** 5 wt %.

With an increase in clay content from 1 to 4 wt %, the storage modulus increases by 1.2 to 1.53 times at -30 °C and 1.56 to 2 times at room temperature (25 °C) in comparison to the pure elastomers. The clay exfoliation in polymer matrix greatly enhances the interfacial area which improves the reinforcement potential. However, this phenomenon can be well explained by

the degree of crystallinity. As supported by XRD, the crystallinity decreases with an increased concentration of clay because of clay platelet exfoliation. This decrease may be attributed to the higher interfacial area and adhesion between the elastomer matrix and exfoliated clay, which reduces the mobility of crystallizable chain segments of elastomer matrix under

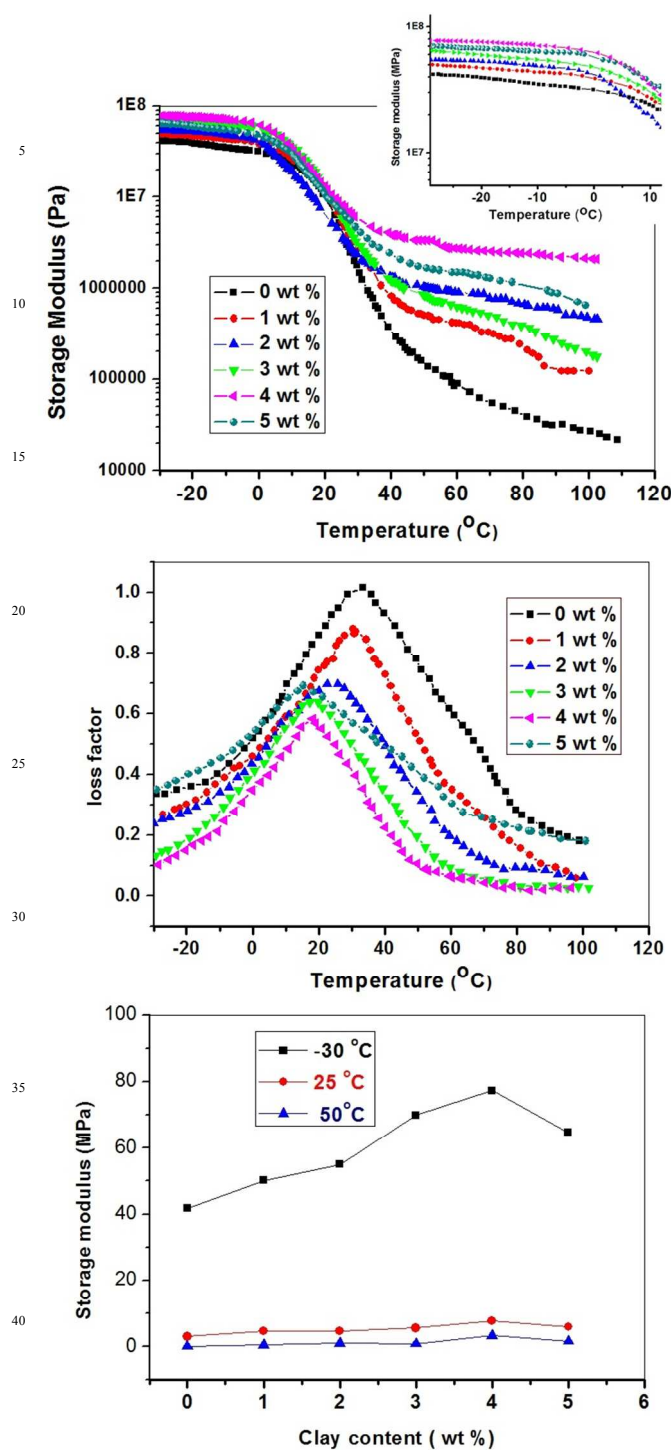


Fig. 7 Dynamic mechanical analysis results, **A.** Variation of storage modulus with temperature, **B.** Variation of loss modulus with temperature & **C.** Variation of storage modulus with clay content at different temperatures

dynamic stress. This results in an enhancement of storage modulus. In the sample having 5 wt % clay, defects or flaws are generated due to the phase separated morphology as observed in FESEM. These initiate micro-cracks under dynamic loading, causes the reduction in storage modulus.

The $\tan \delta$ peak in $\tan \delta$ versus temperature graph denotes the primary relaxation temperature (T_α). The $\tan \delta$ peak designated by $\tan \delta_{\max}$ indicates the maximum dissipation of excitation energy under dynamic stress condition. At primary relaxation temperature or near about it, the chains begin to reptate back and forth along their length. This molecular motion transforms the excitation energy into heat energy. T_α of the pure elastomers is found to be 33.4 °C.

The T_α shifts to a lower temperature with an increase in the filler content in the elastomers. The T_α value decreases from 33.4 °C to 15.4 °C with an increase in filler content from 0 wt % to 5 wt %. This may be attributed to the highly viscous clay dispersed reaction mixture, which affects the initiator diffusion and chain propagation during cationic polymerization. As per previous discussion, the main polymer chain consists of ST and DVB at which linseed oil molecules are grafted. The linseed oil segment of this polymer chain is flexible whereas the ST-DVB segment is rigid. During polymerization reaction, it is also possible that DVB and ST can penetrate more easily in to the layered structure of modified MMT than the long chain triglyceride molecules. This loss of ST and DVB reduces the overall rigidity of nano composites, resulting a decrease in T_α values⁴³.

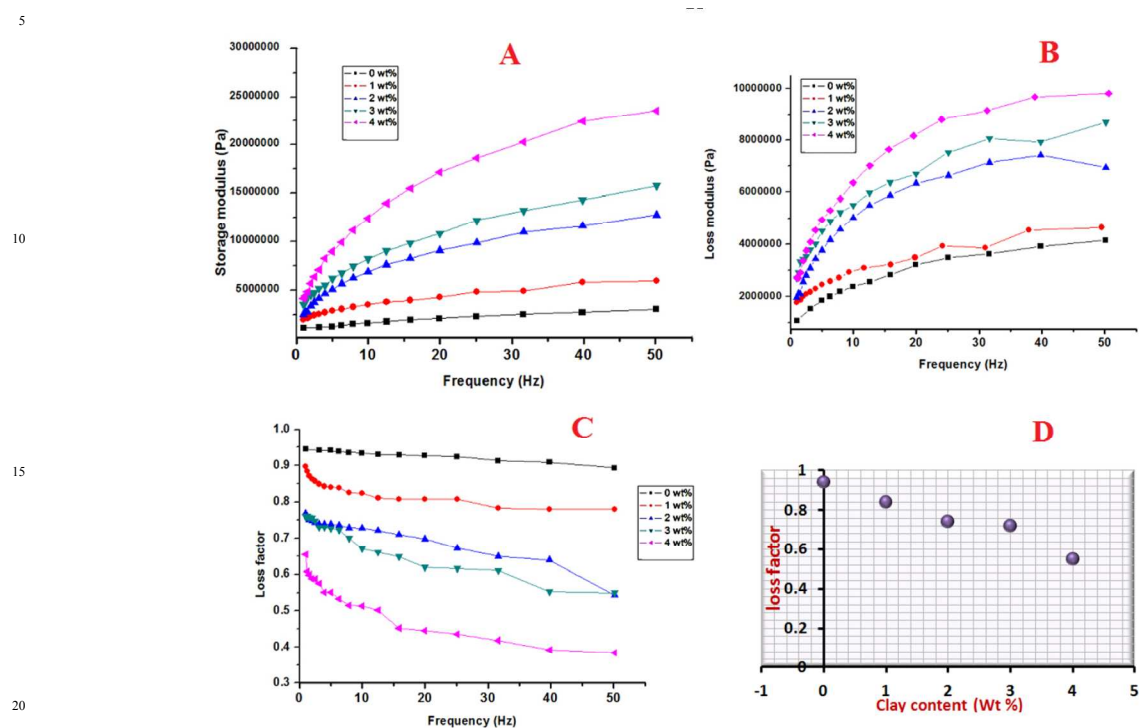
The performance of any damping materials is measured by the loss factor i.e. $\tan \delta$. The variation of $\tan \delta$ as a function of temperature is represented in Figure 7. The $\tan \delta_{\max}$ i.e. the maximum value of the loss factor of different nano composites are in the range of 0.58 to 0.87, whereas the room temperature loss factor $\tan \delta_{rt}$ of different nano composites are in the range of 0.58 to 0.82. The high $\tan \delta$ value ($\tan \delta \geq 0.3$) of materials in a wide temperature (ΔT) range is a prerequisite for any damping applications⁴⁴. The temperature ranges (ΔT) for effective damping ($\tan \delta \geq 0.3$) of different nano composites evaluated from $\tan \delta$ versus temperature curve are listed in Table 2. The temperature ranges for effective damping are in the range of 39 °C to 87 °C. The loss factor values are comparable with the damping properties of different conventional polymeric materials such as Poly (methyl methacrylate) (PMMA), Polytetrafluoroethylene (PTFE), epoxy, neoprene rubber etc⁴⁵. Also, loss factor values are comparable to different polymeric materials such as polymer blend, polymer IPN, polymer composites specially screened for damping applications⁴⁶⁻⁴⁸. A comparison of loss factors of different damping materials with the developed nano composites is shown in Table 3. In addition with this, the relaxation temperatures of different nano composites are around room temperature (25 °C); so they can be effectively applied as damping materials in practical applications.

In the next step, the frequency dependence of storage modulus (E'), loss modulus (E'') and loss factors were examined. The storage modulus, loss modulus and loss factor as a function of frequency are plotted in Figure 8. The dynamic moduli (both E' & E'') grows steeply with an increase in the frequency. The plot of E' versus frequency expresses the frequency response of elasticity. On the other hand, the plot of E'' versus frequency indicates about the frequency response of viscous behaviour. The increase in E' may result from the increase in molecular chain rigidity and the interaction between polymer chains. The increase in E'' arises due to the increase in relative motion between polymer chains. A slight decrease in $\tan \delta$ for nano composites

Table 2 DMA temperature scan results of nano composites

| OMMT content in nano composites (wt %) | T_g (°C) | E' at -30°C (MPa) | E'' at 25 °C (MPa) | $(\tan \delta)_{\max}$ | $(\tan \delta)_{rt}$ | ΔT (°C) |
|--|------------|---------------------|----------------------|------------------------|----------------------|-----------------|
| 0 | 33.4 | 41.7 | 3 | 1.01 | 0.94 | 78 |
| 1 | 30.8 | 50 | 4.7 | 0.87 | 0.82 | 83 |
| 2 | 24.6 | 55 | 4.6 | 0.70 | 0.69 | 67 |
| 3 | 18.4 | 70 | 5.5 | 0.64 | 0.58 | 51 |
| 4 | 17.9 | 77 | 7.7 | 0.58 | 0.49 | 39 |
| 5 | 15.4 | 64 | 6 | 0.68 | 0.62 | 87 |

a

**Fig. 8** DMA frequency sweep measurement of **A.** Storage modulus, **B.** loss modulus, **C.** loss factor & **D.** Variation of loss factor with clay content**Table 3** Review of loss factor of different damping materials

| Materials | X Loss factor at 1 Hz | Reference |
|---------------------------|--------------------------|-----------|
| PMMA | ≈ 0.1 | 45 |
| PTFE | ≈ 0.224 | 45 |
| Epoxy | ≈ 0.039 | 45 |
| Neoprene rubber | ≈ 1.12 | 45 |
| Polymer blends | ≈ 0.2-0.6 | 46 |
| Polymer IPN | ≈ 0.2-0.8 | 47 |
| Polymer composites | ≈ 0.05-0.8 | 48 |
| Developed nano composites | ≈ 0.5-0.9 | |

a

with an increase in frequency is observed, signalling a more elastic like response than viscous response with an increased frequency. The values of $\tan \delta$, E' and E'' at 5 Hz, 10 Hz, 30

Hz and 50 Hz are shown in Table 4. From the frequency response of $\tan \delta$ for nano composites, it is clear that the damping property is stable within the measured frequency range (1 to 50 Hz). It is also identified that the $\tan \delta$ decreases with an increase in clay content. The values of $\tan \delta$ at 5 Hz are plotted as a function of varying clay content in nano composites in Figure 8. The energy dissipated in the polymer matrix is due to the intermolecular friction and molecular chain relaxation. The segmental mobility of polymer chain is greatly restricted by the clay layers, leading to a decrease in the loss factor. Thus the nano composites can be employed effectively in different damping devices like constrained layer damping system (CLD), active constrained layer damping system (ACLSD), hysteresis damper etc to control unwanted vibration and noise in different applications over a wide range of temperature and frequency.

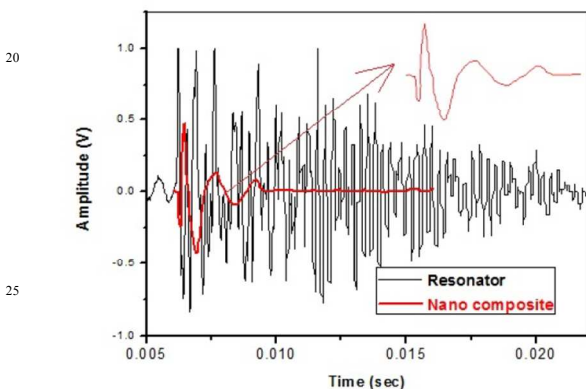
Table 4 Frequency scan results of DMA

| OMMT content in nano composites (wt %) | Storage modulus (MPa) at | | | | Loss modulus (MPa) at | | | | Loss factor at | | | |
|--|--------------------------|-------|-------|-------|-----------------------|-------|-------|-------|----------------|-------|-------|-------|
| | 5 Hz | 10 Hz | 30 Hz | 50 Hz | 5 Hz | 10 Hz | 30 Hz | 50 Hz | 5 Hz | 10 Hz | 30 Hz | 50 Hz |
| 0 | 1.2 | 1.7 | 2.5 | 3 | 1.9 | 2.4 | 3.6 | 4.1 | 0.94 | 0.93 | 0.92 | 0.84 |
| 1 | 3 | 3.6 | 4.8 | 6 | 2.5 | 3 | 3.9 | 4.7 | 0.84 | 0.83 | 0.79 | 0.78 |
| 2 | 5.2 | 6.9 | 10.7 | 12.8 | 3.8 | 5 | 7 | 6.9 | 0.74 | 0.73 | 0.65 | 0.55 |
| 3 | 6.1 | 8.2 | 13 | 15.8 | 4.5 | 5.52 | 8 | 8.7 | 0.72 | 0.67 | 0.61 | 0.54 |
| 4 | 9 | 12.4 | 19.8 | 23.7 | 5 | 6.4 | 9 | 9.8 | 0.55 | 0.51 | 0.42 | 0.38 |

a

5 Attenuation of low frequency vibration using Nano composites

The attenuation of a laboratory generated mechanical vibration (1.5 V, 5 Hz) through the nano composites is studied. In the fabricated testing system, mild steel plate resonator is taken as the reference. With respect to the mild steel, the vibration damping property of the nano composites are evaluated. The time decay waveform of mild steel plate and nano composite are shown in Figure 9. The wave form for nano composite containing 2 wt % filler is taken as the representative waveform of all nano composites. The wave form of mild steel plate exhibits very negligible decay but the nano composite exhibits very sharp decay within two cycles.

**Fig. 9** Time decay wave form of resonator and nano composite

The loss factor of mild steel plate at room temperature (25 °C) at a frequency of 5 Hz is determined as 0.0053; the loss factor of nano composites having different clay compositions are tabled in Table 5. These results are slightly different from the dynamic mechanical results at 5 Hz and at the room temperature (25 °C). In a laboratory investigation of loss factor, it is very difficult to eliminate energy loss due to the external environment. There are some factors that should be considered during this experiment; these are-(1) losses due to attachment of sensing device such as accelerometers and strain gauges, (2) losses due to the excitation of sound waves in the atmosphere, and (3) losses due to the interaction of the sample with the supporting structure such as

clamp⁴⁹. In our experiment, a miniature lightweight (1.8 g) accelerometer was used to eliminate the losses due to the attachment of the accelerometer. The optical vibration sensing device like laser vibrometer is the best solution to eliminate this disturbance. Two long strings were utilized to suspend the test piece for eliminating support related losses. The vibration testing results reveal that the nano composites effectively attenuate the excitation vibration within 2 or 3 cycles, a primary requirement for practical damping applications.

Table 5 Vibration response results of nano composites

| OMMT content in nano composites (wt %) | Loss factor at 5 Hz |
|--|---------------------|
| 0 | 0.82 |
| 1 | 0.73 |
| 2 | 0.69 |
| 3 | 0.56 |
| 4 | 0.51 |

a

Conclusions

Value added engineering nano composites have obtained from linseed oil and organophilic MMT, renewable resources. The XRD analysis reveals a clear decrease in the crystallinity of polymer with an increase in the clay content in nano composites because of clay platelet exfoliation in the polymer matrix. Intercalation of polymer molecules into clay layers formed a homogeneous morphology, observed through FESEM. The 4 wt % of clay is the optimum level that can be incorporated in the polymer matrix. Beyond this optimum level, phase separated morphology was formed. In dynamic mechanical analysis, the storage modulus is increased by 1.56 to 2 times at room temperature (25 °C) with an increase in the clay incorporation from 1 to 4 %. The maximum damping loss factor has the range of 0.58 to 0.87 with a temperature range (ΔT) of 39 °C to 87 °C for effective damping. The nano composites also exhibited effective and stable loss factor in the frequency scan of dynamic mechanical analysis. A successive reinforcing capability of nano clay was identified both in a wide temperature range and low frequency regions. A laboratory generated low frequency vibration is successfully attenuated by nano composites within 2 or 3 cycles; this further establishes that the developed nano composites are preferable candidates for damping applications.

Acknowledgement

The financial support under Technical education quality improvement project (TEQIP), Government of India is highly acknowledged.

Notes and references

^a Address, Department of Polymer Science and Technology, University of Calcutta, 92 APC Road, Kolkata, India. Fax: 03323525106; Tel: 03323525106; E-mail: ppk923@yahoo.com.

^b Address, Precision Metrology Laboratory, Department of Mechanical Engineering, Sant Longowal Institute of Engineering & Technology, Sangrur, Punjab 148106, India. E-mail: rajesh_krs@rediffmail.com.

- 1 A. K. Mohanty, M. Misra and G. Hinrichen, *Macromol. Mater. Eng.*, 2000, **276/277**, 1-24.
- 15 2 J. Lu and R. P. Wool, *J. Appl. Polym. Sci.*, 2006, **99**, 2481-2488.
- 3 S. N. Khot, J. J. Lascala, E. Can, S. S. Morye, G. I. Williams, G. R. Palmese, S. H. Kusefoglu and R. P. Wool, *J. Appl. Polym. Sci.*, 2001, **82**, 703-723
- 20 4 Y. Lu and R. C. Larock, *Biomacromolecules*, 2007, **8**, 3108-3114.
- 5 Y. Lu and R. C. Larock, *Macromol. Mater. Eng.*, 2007, **292**, 1085-1094.
- 6 S.S. Ray and M. Bousmina, *Progr. Mater. Sci.*, 2005 **50**, 962.
- 25 7 P.B. Messerith and E.P. Giannelis, *J. Polym. Sci. Part A: Polym. Chem.*, 1995, **33**, 1047.
- 8 M. Okamoto, *Mater. Sci. Technol. Lond.*, 2006, **2**, 756-779.
- 9 V. C. Divya, V. V. Pattanshetti, R. Suresh and R. R. N. Sailaja, *J. Polym. Res.*, 2013 **20**, 51.
- 30 10 E. P. Giannelis, *Adv. Mater.*, 1996, **8**, 29-35.
- 11 D.R. Paul and L.M. Robeson, *Polymer*, 2008, **49**, 3187-3204.
- 12 M. Ahmed Youssef, *polym-plast technol*, 2013, **52**, 635-660.
- 13 V. Mittal, *Optimization of Polymer Nanocomposite Properties*, John Wiley & Sons, USA, 2009.
- 35 14 F. Li and R. C. Larock. *J. Appl. Polym. Sci.* 2001, **80**, 658-670.
- 15 F. Li, A. Perrenoud and R. C. Larock. *Polymer*, 2001, **42**, 10133-10145.
- 16 R. P. Wool, *Chem Tech*, 1999, **29**, 44-48.
- 40 17 A. Guo, I. Javni and Z. S. Petrovic., *J. Appl. Polym. Sci.* 2000, **77**, 467-473.
- 18 Z. S. Petrovic, M. J. Cevallos, I. Javni, D. W. Schaefer and R. Justice, *J. Polym. Sci. Part B: Polym. Phys.*, 2005, **43**, 3178-3190.
- 45 19 A. Rybak, P. A. Fokou and M. A. R. Meier, *Eur. J. Lipid Sci. Technol.*, 2008, **110**, 797-804.
- 20 P. H. Henna and R. C. Larock, *Macromol Mater Eng.*, 2007, **292**, 1201-1209.
- 21 Y. Xia, Y. Lu and R. C. Larock, *Polymer*, 2010, **51**, 53-61.
- 50 22 M. A. Mosiewicki, I. Mirta and A. Aranguren, *Eur. Polym. J.* 2013, **49**, 1243-1256.
- 23 S.G. Tan, Z. Ahmad and W.S. Chow, *Appl. Clay Sci.*, 2014, **90**, 11-17.
- 115 24 B. Songa, W. Chenb, Z. Liuc and S. Erhanc, *Int. J. Plast.*, 2006, **22**, 1549-1568.
- 55 25 S. Sen and G. Cayli, *Polym. Int.* 2010, **59**, 1122-1129.
- 26 H. Uyama, M. Kuwabara, T. Tsujimoto, M. Nakano, A. Usuki and S. Kobayashi, *Chem. Mater.* 2003, **15**, 2492-2494.
- 27 M. M. Reddy, S. Vivekanandhan, M. Misra, S. K. Bhatia and A. K. Mohanty, *Prog. Polym. Sci.*, 2013, **38**, 1653-1689.
- 60 28 M. J. John and S. Thomas, *Carbohydr. Polym.* 2008, **71**, 343-364.
- 29 D. P. Pfister and R. C. Larock, *J. Appl. Polym. Sci.*, 2012, **123**, 1392-1400.
- 65 30 R. L. Quirino, J. Woodford and R. C. Larock, *J. Appl. Polym. Sci.*, 2012, **124**, 1520-1528.
- 31 R. L. Quirino and R. C. Larock, *J. Appl. Polym. Sci.*, 2011, **121**, 2039-2049.
- 32 D. P. Pfister and R. C. Larock, *J. Appl. Polym. Sci.*, **2013**, 127, 1921-1928.
- 33 R. Das, R. Kumar and P. P. Kundu, *J. Appl. Polym. Sci.*, 2013, **130**, 3611-3623.
- 34 R. Das, R. Kumar and P. P. Kundu, 2014, **Article ID** 840397.
- 35 E. Riande, R. Diaz-Calleja, M. Prolongo, R. Masegosa and C. Salom, *Polymer viscoelasticity: stress and strain in practice*, 2000, Marcel Dekker, Inc, New York.
- 75 36 D. I. G. Jones, *Handbook of Viscoelastic Vibration Damping*; 2001, Wiley Inter science, New York.
- 37 B. H. Hameed, L. F. Lai, and L. H. Chin, *Fuel Processing Technology*, 2009, **90**, 606-610.
- 80 38 W. DeSilva, 2007, *Vibration Damping, Control and Design*, CRC Press.
- 39 L. Hao, Y. Yu and Y. Yang, *Eur. Polym. J.*, 2005, **41**, 2016-2022.
- 85 40 H. Yang, J. Irudayaraj and M. M. Paradkar, *Food Chem.*, 2005, **93**, 25-32.
- 41 G. Kumar, N. Nisha, S. Mageswari and K. Subramanian, *J Polym Res*, 2011, **18**, 241-250.
- 42 L. Wang and A. Wang, *J. Hazard. Mater.*, 2008, **160**, 173-180.
- 43 J. Lu, C. K. Hong and R. P. Wool, *J. Polym. Sci. Part B: Polym. Phys.*, 2004, **42**, 1441.
- 44 T. Trakulsujaritchook and D. J. Hourston, *Eur. Polym. J.*, 2006, **42**, 2968.
- 95 45 D. D. L. Chung, *J Alloys Compd*, 2003, **355**, 216-223.
- 46 X. Lu, X. Li and M. Tian, *Polym. Adv. Technol.*, 2014, **25**, 21-28.
- 47 C.-L. Qin, W.-M. Cai, J. Cai, D.-Y. Tang, J.-S. Zhang and M. Qin, *Mater. Chem. Phys.* 2004, **85**, 402.
- 100 48 I. C. Finegan, R. F. Gibson, *Compos. Struct.*, 1999, **44**, 89-98.
- 49 D.L. Russel, "Remarksonexperimental determination of modal damping rates in elastic beams," in *Vibration and Damping in Distributed Systems-WKB and Wave Methods, Visualization and Experimentation*, G. Chen and J. Zhou, Eds., **volume. 2, chapter 5**, 1993, CRC Press, Tokyo, Japan.